DR#0420-0

DOE/MC/21179-2335
(DE87001100)

Energy

FOSSIL

Rock Matrix and Fracture Analysis of Flow in Western Tight Gas Sands

1986 Annual Report

N.R. Morrow
J.S. Buckley
S.M. Cather
K.R. Brower
V. Dandge
M. Graham
B. Gonzales

February 1987

Work Performed Under Contract No.: DE-AC21-84MC21179

For
U.S. Department of Energy
Office of Fossil Energy
Morgantown Energy Technology Center
Morgantown, West Virginia

By
New Mexico Petroleum Recovery Research Center
New Mexico Institute of Mining and Technology
Socorro, New Mexico

DISCLAIMER

This report was prepared as an account of work sponsored by an agency of the United States Government. Neither the United States Government nor any agency thereof, nor any of their employees, makes any warranty, express or implied, or assumes any legal liability or responsibility for the accuracy, completeness, or usefulness of any information, apparatus, product, or process disclosed, or represents that its use would not infringe privately owned rights. Reference herein to any specific commercial product, process, or service by trade name, trademark, manufacturer, or otherwise does not necessarily constitute or imply its endorsement, recommendation, or favoring by the United States Government or any agency thereof. The views and opinions of authors expressed herein do not necessarily state or reflect those of the United States Government or any agency thereof.

This report has been reproduced directly from the best available copy.

Available from the National Technical Information Service, U. S. Department of Commerce, Springfield, Virginia 22161.

Price: Printed Copy A03
Microfiche A01

Codes are used for pricing all publications. The code is determined by the number of pages in the publication. Information pertaining to the pricing codes can be found in the current issues of the following publications, which are generally available in most libraries: *Energy Research Abstracts (ERA); Government Reports Announcements* and Index *(GRA* and I); *Scientific and Technical Abstract Reports (STAR);* and publication NTIS-PR-360 available from NTIS at the above address.

Printed in the United States of America
USDOE Office of Scientific and Technical Information
Oak Ridge, Tennessee

DISCLAIMER

Portions of this document may be illegible in electronic image products. Images are produced from the best available original document.

DOE/MC/21179--2335
(DE87001100)

FOSSIL ENERGY

Rock Matrix and Fracture Analysis of Flow in Western Tight Gas Sands

1986 Annual Report

DOE/MC/21179--2335

DE87 001100

N.R. Morrow
J.S. Buckley
S.M. Cather
K.R. Brower
V. Dandge
M. Graham
B. Gonzales

February 1987

Work Performed Under Contract No.: DE-AC21-84MC21179

For
U.S. Department of Energy
Office of Fossil Energy
Morgantown Energy Technology Center
Morgantown, West Virginia

By
New Mexico Petroleum Recovery Research Center
New Mexico Institute of Mining and Technology
Socorro, New Mexico

TECHNICAL INFORMATION CENTER
OFFICE OF SCIENTIFIC AND TECHNICAL INFORMATION
UNITED STATES DEPARTMENT OF ENERGY

DOE/MC/21179-2335
(DE87001100)
Distribution Category UC-132

Rock Matrix and Fracture Analysis of Flow in Western Tight Gas Sands

1986 Annual Report

N.R. Morrow
J.S. Buckley
S.M. Cather
K.R. Brower
V. Dandge
M. Graham
B. Gonzales

Work Performed Under Contract No.: DE-AC21-84MC21179

For
U.S. Department of Energy
Office of Fossil Energy
Morgantown Energy Technology Center
P.O. Box 880
Morgantown, West Virginia 26507-0880

By
New Mexico Petroleum Recovery Research Center
New Mexico Institute of Mining and Technology
Socorro, New Mexico 87801

MASTER

February 1987

TABLE OF CONTENTS

List of Tables iii

List of Figures iv

Acknowledgements v

Executive Summary 1

Background 1

Project Tasks - Year 2 1
Advanced Core Analysis 1
Natural Fractures in Tight Sandstones 1
Effect of Core Handling on Properties of Low Permeability Sands ... 1
Effect of Overburden Pressure on Pore Structure 1

Publications 2

Introduction 2

1. Advanced Core Analysis 2

Screening Tests for Multi-Well Core Samples 2
(a) Adsorption-Desorption Isotherms 5
(b) Surface Area Measurements 5
(c) Index of Quality of Pore Space From Point Counts on Thin Sections 16

2. Natural Fractures in Tight Sandstones 16

Origin of Natural and Artificial Fractures in MWX Sandstones 16

Flow Along Mineralized Fractures 18

3. Effect of Core Handling on Properties of Low Permeability Sands 24

4. Effect of Overburden Pressure on Pore Structures 27

Resin Injection for Visible, UV Microscopy and Electron Microscopy 27

Summary and Future Work 31

Proposed Work for Year 3 32

Task 1. Advanced Core Analysis 32

Task 2. Natural Fractures 33

Task 3. Investigation of Pore-Filling Cements and the Effect of Chemical Treatments on Core Properties 33

Task 4. Effect of Water of Gas Production 34

References 35

LIST OF TABLES

Table 1. Multi-Well Samples 3

Table 2. Permeabilities, Porosities and Surface Areas of Multi-Well Samples on Hand 4

Table 3. Pore Quality in Multi-Well Sandstones and Other Selected Media 17

Table 4. Relative Permeabilities to Nitrogen Gas at Different Levels of Water Saturation 19

LIST OF FIGURES

Figure 1. Desorption-adsorption isotherms (base weight at 20% relative humidity and 25°C unless indicated otherwise)..... 6

Figure 2. Desorption-adsorption isotherms (base weight at 20% relative humidity and 25°C)..... 7

Figure 3. Desorption-adsorption isotherms (base weight at 20% relative humidity and 25°C)..... 8

Figure 4. Desorption-adsorption isotherms (base weight at 20% relative humidity and 25°C)..... 9

Figure 5. Desorption-adsorption isotherms (base weight at 20% relative humidity and 25°C)..... 10

Figure 6. Surface area versus outgassing temperature for sample of MWX1 42-25..... 11

Figure 7. Relationship between nitrogen adsorption and partial pressure (BET plot)..... 13

Figure 8. Adsorption-desorption hysteresis loop for nitrogen on MWX1 42-25..... 14

Figure 9. Effects of sample segregation on surface area..... 15

Figure 10. Permeability to gas versus confining pressure at five levels of water saturation..... 20

Figure 11. Permeability versus confining pressure at five levels of water saturation..... 21

Figure 12. Permeability to gas versus water saturation..... 22

Figure 13. Permeability to gas versus water saturation..... 23

Figure 14. Comparison of water and brine permeabilities..... 25

Figure 15. Permeability to gas versus confining pressure of five levels of water saturation for preserved core (duplicate tests) 26

Figure 16. Gas permeability versus confining pressure at different levels of water saturation for preserved and oven-dried MWX3 42-4 28

Figure 17. Relative permeability to nitrogen as a function of established water saturation at confining pressures of 500 and 5000 psi for preserved and oven-dried MWX3 42-4..... 29

Figure 18. Desorption-adsorption isotherms for MWX3 42-4 (base weight at 20% relative humidity and 25°C)..... 30

ACKNOWLEDGEMENTS

The assistance of Allan Sattler of Sandia Laboratories in the selection and provision of cores used in this study and Vijaya Dandge and Mary Graham in performing the laboratory work is greatly appreciated.

EXECUTIVE SUMMARY

BACKGROUND

The objective of this project is to develop reliable core analysis techniques for tight gas sands; these are essential to proper formation evaluation. The study is mainly concerned with the dependence of flow in tight gas sands on water saturation and confining pressure. This dependency is to be related to the detailed pore structure of tight sands as typified by cores recovered in the Multi-Well experiment.

PROJECT TASKS - Year 2

Advanced Core Analysis

Advanced core analysis includes: porosity measurements (thin section vs. volumetric measurements), Klinkenberg permeability measurements, water adsorption and desorption isotherms, surface area measurements, x-ray analysis, effects of overburden pressure, mineral analysis, and pore structure. Special emphasis has been placed on comparison of thin section porosity to porosity to pore volume and development of a measure of quality of pore space. This approach to quantitative assessment of the quality of reservoir rocks is likely to have wide application.

Natural Fractures in Tight Sandstones

Natural fractures play a dominant role in production from tight sands. The most readily detected fractures in whole core samples are mineralized, the majority being filled by calcite. All available thin sections (about 600 in all) and MWX core on hand have been screened for the presence of natural fractures. Relative permeabilities to gas along healed (calcite-filled) fractures have been determined for two core samples at five levels of water saturation and three levels of overburden pressure (500, 2000 and 5000 psi). Gas relative permeabilities of a core containing a healed fracture (calcite-filled) running along the length of the core have been measured. Results show that the calcite filled fractures heal to where they have roughly the same permeability as the matrix, although some differences in the pressure sensitivity of the fracture and the matrix were observed.

Effect of Core Handling on Properties of Low Permeability Sands

Permeabilities for fresh cores (not allowed to dry out) are compared with results for conventional (dried) cores to determine what changes result from drying. Results obtained to date show that drying can affect the permeability and relative permeabilities of tight gas sands but the effect is not serious. Further capillary pressure measurements have been obtained from both high speed centrifuge and desorption isotherm data.

Effect of Overburden Pressure on Pore Structure

UV microscopy is being employed to examine much finer features of pore structure (of the order of a few tenths microns) than is possible by conven-

tional petrographic microscopy. A formulation of low viscosity resin containing both visible and UV dye has been developed. Comparison of pore structure of a low permeability gas sand at ambient pressure with that at 5000 psi confining pressure supports a previous conclusion that sheet pores at grain boundaries tend to close up with increase in overburden pressure.

PUBLICATIONS

During the past year the following articles on the properties of tight sands have appeared or been accepted for publication.

1. Wei, K., Morrow, N.R., and Brower, K.R., "Effect of Fluid, Confining Pressure, and Temperature on Absolute Permeabilities of Low Permeability Sandstones," SPE Formation Evaluation (August 1986) 1, 413-423.

2. Ward, J.S. and Morrow, N.R., "Capillary Pressures and Gas Relative Permeabilities of Low Permeability Sandstone," SPE 13882 presented at the 1985 SPE/DOE Symposium on Low Permeability Reservoirs, Denver, CO, May 19-22, 1985; SPE Formation Evaluation, In press.

3. Kilmer, N.H., Morrow, N.R., and Pitman, J.K., "Pressure Sensitivity of Low Permeability Sandstones," Journal of Petroleum Science and Engineering, In press, 1987.

INTRODUCTION

This report presents progress for the second year of a five-year project concerned with the pore structure and flow properties of low permeability gas sands. The main objective of work during the first year was to carry out advanced core analysis on cores recovered from the Multi-Well Field Experiment. In Phase II, the properties of both fractured and non-fractured samples (hereafter referred to as matrix) have been studied. Special attention was given to the combined effect of overburden pressure and water saturation on gas flow. The project is on schedule.

1. ADVANCED CORE ANALYSIS

Screening Tests for Multi-Well Core Samples

The status of advanced core analysis work on 35 rock matrix core samples from selected zones of Multi-Wells 1, 2, and 3 is summarized in Table 1. Measurements of the effect of confining pressure on permeability were made for first unloading at pressures of 5000, 2000, and 500 psi, with Klinkenberg permeabilities being determined at 5000 and 500 psi (see Table 2). Results for cores classified by well and zone were presented previously.[1] Estimates of pore size shown in Table 2 were obtained from the slope of plots of permeability vs. mean pore pressure. The ratios of $k_{\infty,500}/k_{\infty,5000}$ ranged from 1.5 to 44.4; thus, the tested cores represent a wide range of sensitivities of permeability to overburden pressure.

Table 1. Multi-Well Samples

Well	ID	Depth (ft.)	Geologic Zone	Gas Permeability Screening Tests*	Relative Permeability	Adsorption-Desorption Core A†	Adsorption-Desorption Core B††	Surface Area	Clay Analysis	Pore Cast	Thin Section
MWX-1	3-11	4319.4-4320.4	PAR							X	X
MWX-1	3-21	4308.3-4309.1	PAR							X	X
MWX-1	8-16	4548.4-4548.9	FM	X			X			X	X
MWX-1	10-13	4699.7-4700.5	FM	X		X		X	X	X	X
MWX-1	13-15	4851.0-4851.5	FM	X			X	X			X
MWX-1	22-20	5357.2-5357.7	FP	X		X	X	X	X	X	X
MWX-1	29-24	5725.7-5726.6	FP	X			X	X		X	X
MWX-2	17-22	4937.0-4937.8	FM	X		X	X	X	X	X	X
MWX-2	47-34	4195.5-4916.6	FM	X		X	X	X	X	X	X
MWX-1	14-24A	4917.9-4918.2	FM	X			X	X		X	X
MWX-1	14-24B	4918.2-4918.9	FM	X			X	X		X	
MWX-3	58-14	4918.1-4918.7	FM	X		X		X	X	X	X
MWX-3	60-19	5726.3-5726.8	FP	X		X		X	X	X	
MWX-3	63-16	5832.1-5832.6	FP	X			X	X		X	X
MWX-3	64-29	6464.5-6465.0	CO	X	X	X		X		X	
MWX-3	66-17	6893.4-6893.8	PAL	X	X	X		X		X	X
MWX-3	67-16	7096.1-7096.7	PAL	X	X	X		X		X	X
MWX-3	67-35	7134.2-7134.6	PAL	X	X	X		X		X	X
MWX-3	68-15	7551.2-7551.7	SH							X	X
MWX-1	3-25	4330.7-4331.6	PAR	X		X		X		X	X
MWX-1	A-CO	6402.1-6402.7	CO	X			X	X	X	X	X
MWX-1	B-CO	6435.3-6436.1	CO	X			X	X	X		X
MWX-1	C-CO	6502.7-6503.2	CO	X			X	X			X
MWX-1	D-CO	6536.5-6537.1	CO	X			X	X	X		X
MWX-2	E-CO	6432.6-6433.2	CO	X			X	X			X
MWX-2	F-CO	6452.0-6453.0	CO	X			X	X			X
MWX-2	G-CO	6471.8-6472.3	CO	X			X	X			X
MWX-2	H-CO	6507.4-6508.0	CO	X			X	X		X	X
MWX-2	I-CO	6537.0-6537.9	CO	X			X	X	X	X	X
MWX-2	J-PAL	7119.4-7120.3	PAL	X			X	X		X	X
MWX-2	K-PAL	7139.2-7139.9	PAL	X			X	X	X	X	X
MWX-2	L-PAL	7278.9-7279.7	PAL	X			X	X		X	X
MWX-3	M-CO	6445.0-6445.8	CO	X			X	X	X		X
MWX-3	N-CO	6461.1-6461.8	CO	X			X	X			
MWX-3	R-CO	6511.9-6512.4	CO	X			X	X			

Key to geologic zone: CO = Coastal; FM = Fluvial (Meander Belts); FP = Fluvial (Point Bars); PAL = Paludal; PAR = Paralic; SH = Shoreline/Marine

X - denotes work completed

*Measurements done for first unloading cycle and at 5000, 2000, 500 psi confining pressure.
†Oven-dried core.
††Humidified core.

Table 2. Permeabilities, Porosities and Surface Areas of Multi-Well Samples on Hand.

Sample		Geologic Zone	Depth (ft)	Porosity (%)	Surface Area Crushed Samples		Permeability (md) For First Unloading		Estimated Crack Thickness (μm)		$k_{\infty,500}$ / $k_{\infty,5000}$
					m^2/g	m^2/cc (pv)	$k_{\infty,500}$	$k_{\infty,5000}$	at 500 psi	at 5000 psi	
MWX-1	8-16	Fluvial	4548.4-4548.9	5.93	2.54	106.8	14.22	0.484	0.269	0.0602	29.38
MWX-1	10-13*	Fluvial	4699.7-4700.5	6.15	1.30	52.6	14.20	1.02	0.228	0.0575	13.92
MWX-1	13-15	Fluvial	4851.0-4851.5	3.88	1.98	130.0	1.262	0.0353	0.203	0.0371	35.75
MWX-1	22-20	Fluvial	5357.2-5357.7	5.07	1.36	67.5	3.84	0.0855	0.204	0.0455	44.91
MWX-1	29-24	Fluvial	5725.7-5726.6	8.73	1.74	48.2	30.54	3.05	0.286	0.0967	10.01
MWX-1	14-24A	Fluvial	4917.9-4918.2	4.59	0.97	53.4	3.187	0.0718	0.167	0.043	44.39
MWX-1	14-24B	Fluvial	4918.2-4918.9	5.17	0.98	47.6	12.34	1.047	0.335	0.0986	11.79
MWX-1	A-CO	Coastal	6402.1-6402.7	6.70	1.12	41.3	11.3	1.02	0.273	0.0934	11.08
MWX-1	B-CO	Coastal	6435.3-6436.1	6.69	1.27	46.9	5.67	0.623	0.178	0.0554	9.10
MWX-1	C-CO	Coastal	6502.7-6503.2	4.62	2.00	109.4	1.16	0.164	0.0814	0.0399	7.07
MWX-1	D-CO	Coastal	6536.5-6537.1	6.48	1.94	74.2	5.34	0.959	0.167	0.0640	5.57
MWX-2	17-22	Fluvial	4937.0-4937.8	7.49	1.44	47.1	7.28	0.784	0.195	0.0725	9.29
MWX-2	47-34	Fluvial	4915.5-4916.6	7.83	1.07	33.4	46.80	10.30	0.308	0.235	4.54
MWX-2	E-CO	Coastal	6432.6-6433.2	5.94	2.13	89.4	2.13	0.224	0.116	0.0393	9.51
MWX-2	F-CO	Coastal	6452.0-6453.0	6.76	1.50	54.8	13.5	1.43	0.270	0.0929	9.44
MWX-2	G-CO	Coastal	6471.8-6472.3	6.94	1.79	63.6	2.84	0.593	0.086	0.0501	4.79
MWX-2	H-CO	Coastal	6507.4-6508.0	6.76	1.41	51.5	8.54	1.28	0.183	0.0782	6.67
MWX-2	I-CO	Coastal	6537.0-6537.9	6.86	1.50	54.0	17.7	1.98	0.399	0.0863	8.94
MWX-2	J-PAL	Paludal	7119.4-7120.3	9.24	2.15	56.0	6.19	1.89	0.133	0.0809	3.28
MWX-2	K-PAL	Paludal	7139.2-7139.9	5.73	1.94	84.6	2.62	0.125	0.132	0.0292	20.96
MWX-2	L-PAL	Paludal	7278.9-7279.7	5.70	1.44	63.1	0.648	0.169	0.125	0.0453	3.86
MWX-3	58-14	Fluvial	4918.1-4918.7	5.04	2.97	148.3	17.9	0.708	0.403	0.078	25.28
MWX-3	60-19*	Fluvial	5726.3-5726.8	9.39	2.80	71.6	44.3	7.43	0.327	0.128	5.96
MWX-3	63-16	Fluvial	5832.1-5832.6	6.51	3.11	118.4	10.01	0.774	0.216	0.0731	12.93
MWX-3	M-CO	Coastal	6445.0-6445.8	5.77	3.57	154.5	3.448	0.348	0.124	0.0394	9.91
MWX-3	N-CO	Coastal	6461.1-6461.8	7.12	3.46	119.6	11.241	1.568	0.184	0.0827	7.17
MWX-3	R-CO	Coastal	6511.9-6512.4	5.44	3.05	140.5	6.804	0.749	0.144	0.0536	9.08
MWX-3	64-29*	Coastal	6464.5-6465.0	8.64	4.35	121.9	10.31	2.105	0.273	0.196	4.90
MWX-3	66-17*	Paludal	6893.4-6893.8	3.02	2.41	205.1	0.0696	0.0257	0.0517	0.0341	2.71
MWX-3	67-16*	Paludal	7096.1-7096.7	10.35	3.41	78.3	7.86	3.62	0.111	0.097	2.17
MWX-3	67-35*	Paludal	7134.2-7134.6	11.83	3.00	59.3	17.22	11.15	0.195	0.210	1.54

*Starred measurements are for samples oven-dried at 110°C; others dried at 45% relative humidity and room temperature.

In carrying out studies of topics such as sensitivity of permeability to confining pressure, relative permeabilities, capillary pressures, pore structure, the effects of drying conditions and chemical treatments etc., the results given in Table 2 provided the basis for selecting suites of cores having a desired range of properties.

During the past year advanced core analysis work has been concentrated in the following areas:

(a) Adsorption-desorption isotherms.
(b) Surface area measurements.
(c) Index of quality of pore space from point counts on thin sections.

Other work which falls within the broad category of advanced core analysis is also contained in this report. Work on fractured cores is described under Task 2, and the effects of drying preserved field samples under Task 3 and high speed centrifuge capillary measurements under Task 4.

(a) Adsorption-Desorption Isotherms

Measurements of desorption-adsorption isotherms have been completed for all the Multi-Well samples on hand. The data are presented in Figs. 1-5 by well number and geologic zone. The results are presented on the basis of weight given at 20% relative humidity and 25°C. Prior to the experiment, the cores were dried at 45% relative humidity and 25°C, except when the cores were oven-dried at 110°C, as indicated.

All samples showed hysteresis with pressures for desorption being higher than those for adsorption, as would be expected of a capillary condensation mechanism. The fluvial samples showed a relatively wide range of behavior. The results indicate that from 10% to 50% of pore space consists of microporosity with pore sizes of less than 10 nm (this pore size corresponds to 90% relative humidity)[2] (see Figs. 1-3). Nine coastal samples were tested. They were found to cover a smaller range than the fluvial samples (see Figs. 4-5) with saturations at 90% relative humidity ranging from about 15% to 35%.

Further work will involve comparison of water adsorption behavior with BET measurement of surface area. The reservoir can be expected to be at very close to 100% relative humidity. In general the quality of the reservoir rock will be inversely proportional to its adsorption capacity at high relative humidity. Thus adsorption measurements provide a simple method of measuring the quality of a reservoir rock and the volume of microporosity associated with pores smaller than a given size.

(b) Surface Area Measurements

A relationship was noted previously[6] between surface-area-per-unit pore volume and the amount of water held at surfaces by adsorption or capillarity in very small pores, as revealed by water vapor adsorption/desorption measurements. This has prompted a more detailed look at the significance of surface area as determined by BET measurements for tight gas core samples since these may provide a useful indication of how much pore volume is in the form of microporosity. Fig. 6 shows the relationship between outgassing temperature and measured surface area for several crushed samples from MWX1 42-25. These

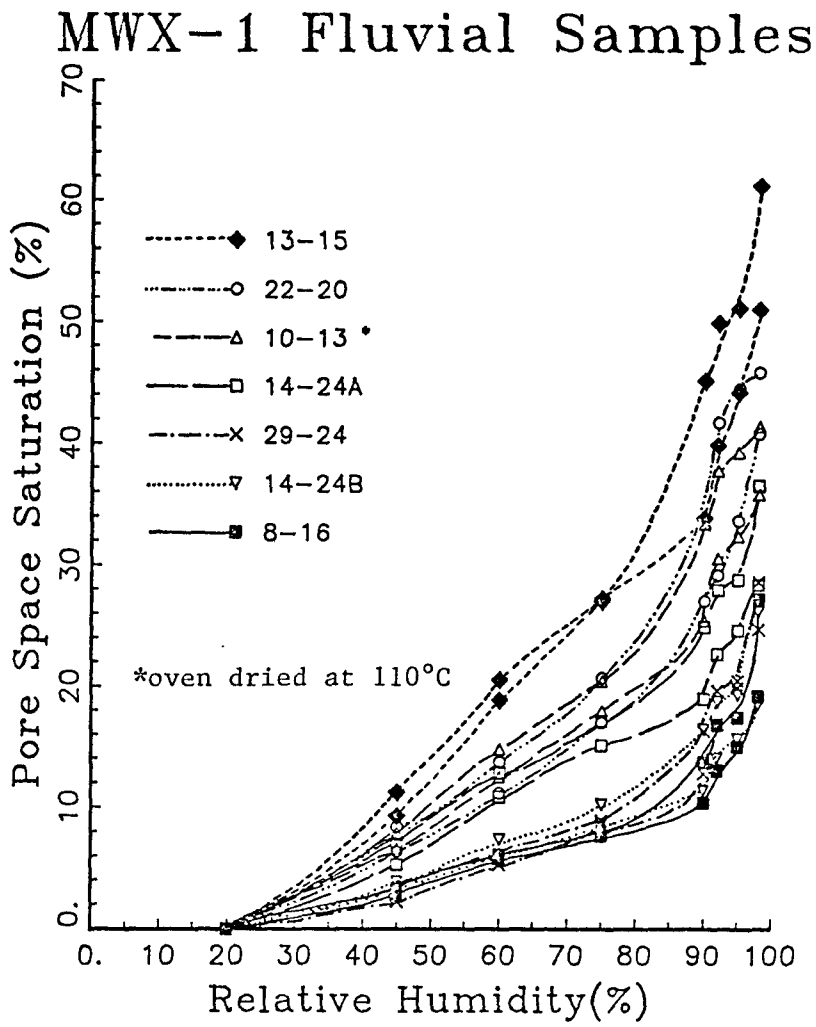

Figure 1. Desorption-adsorption isotherms (base weight at 20% relative humidity and 25°C unless indicated otherwise).

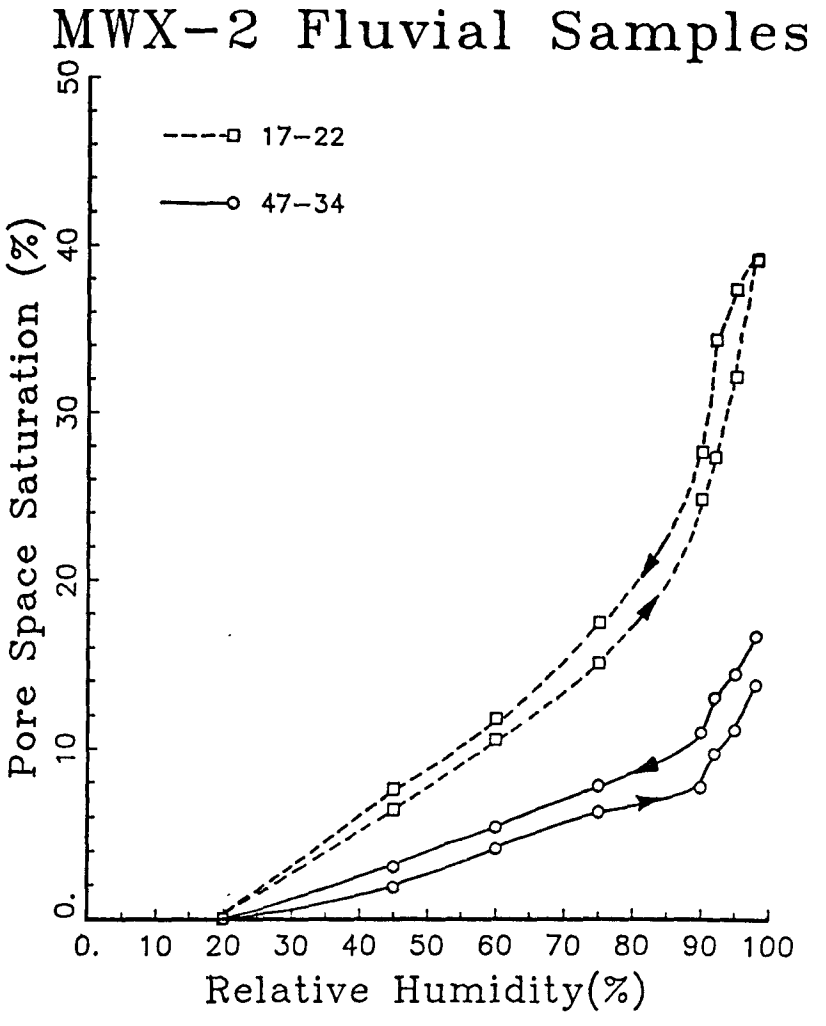

Figure 2. Desorption-adsorption isotherms (base weight at 20% relative humidity and 25°C).

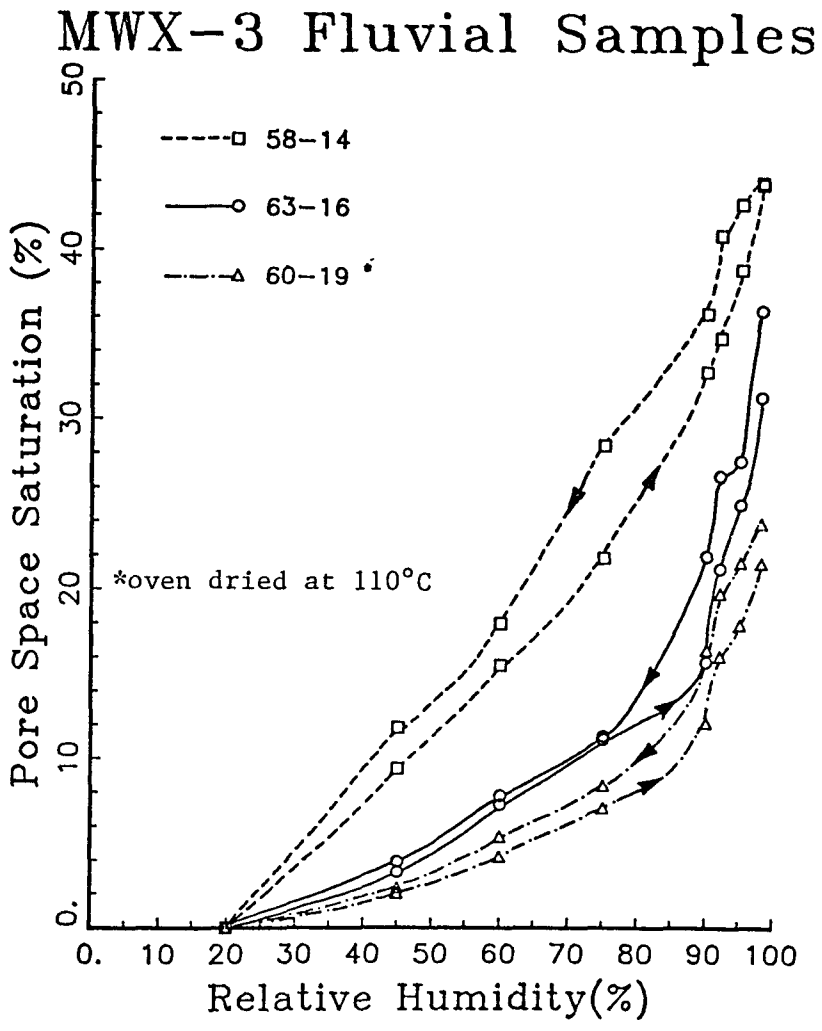

Figure 3. Desorption-adsorption isotherms (base weight at 20% relative humidity and 25°C).

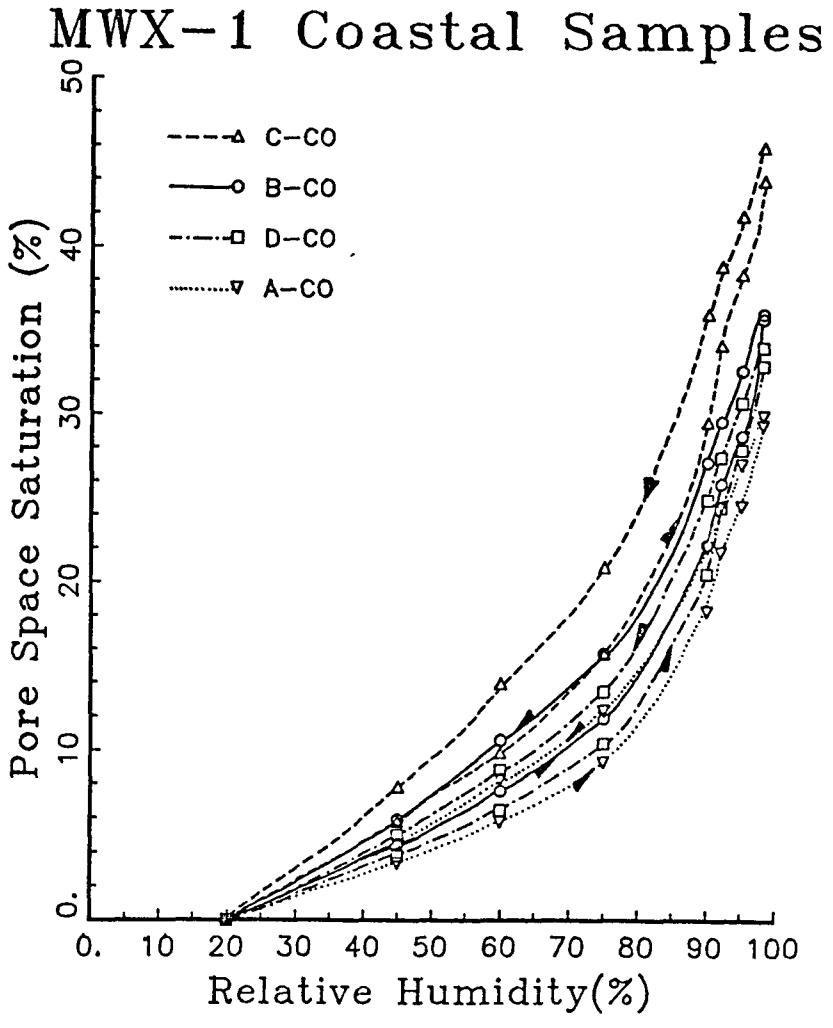

Figure 4. Desorption-adsorption isotherms (base weight at 20% relative humidity and 25°C).

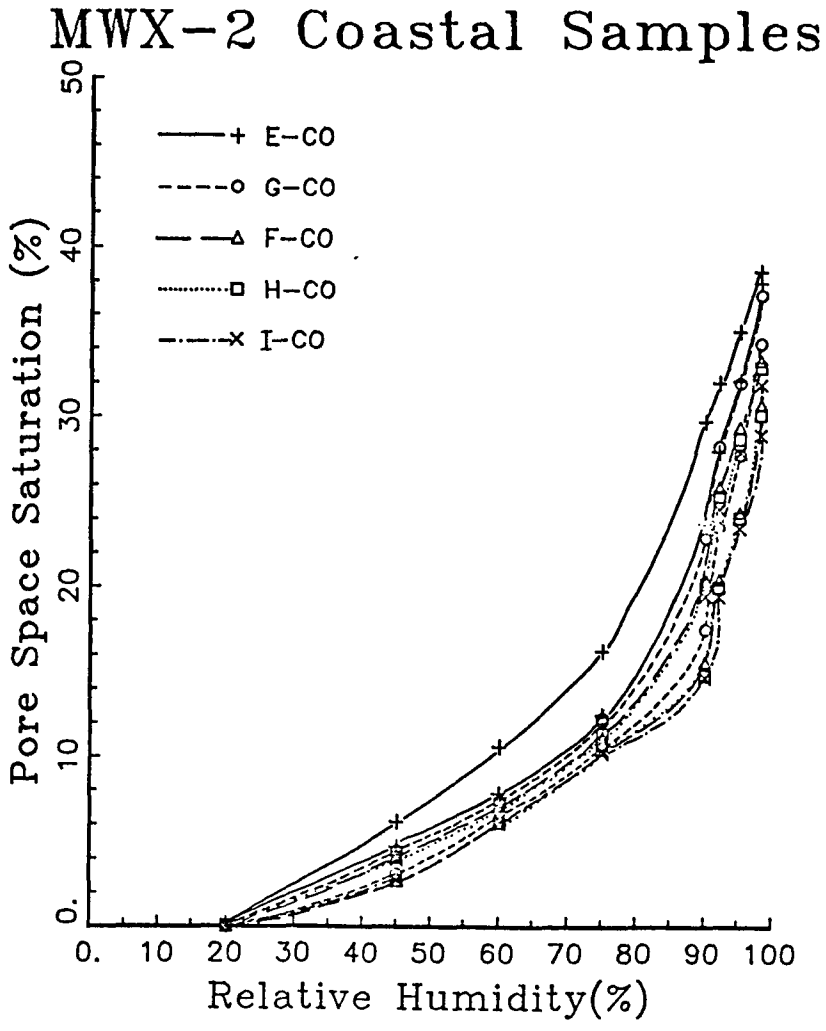

Figure 5. Desorption-adsorption isotherms (base weight at 20% relative humidity and 25°C).

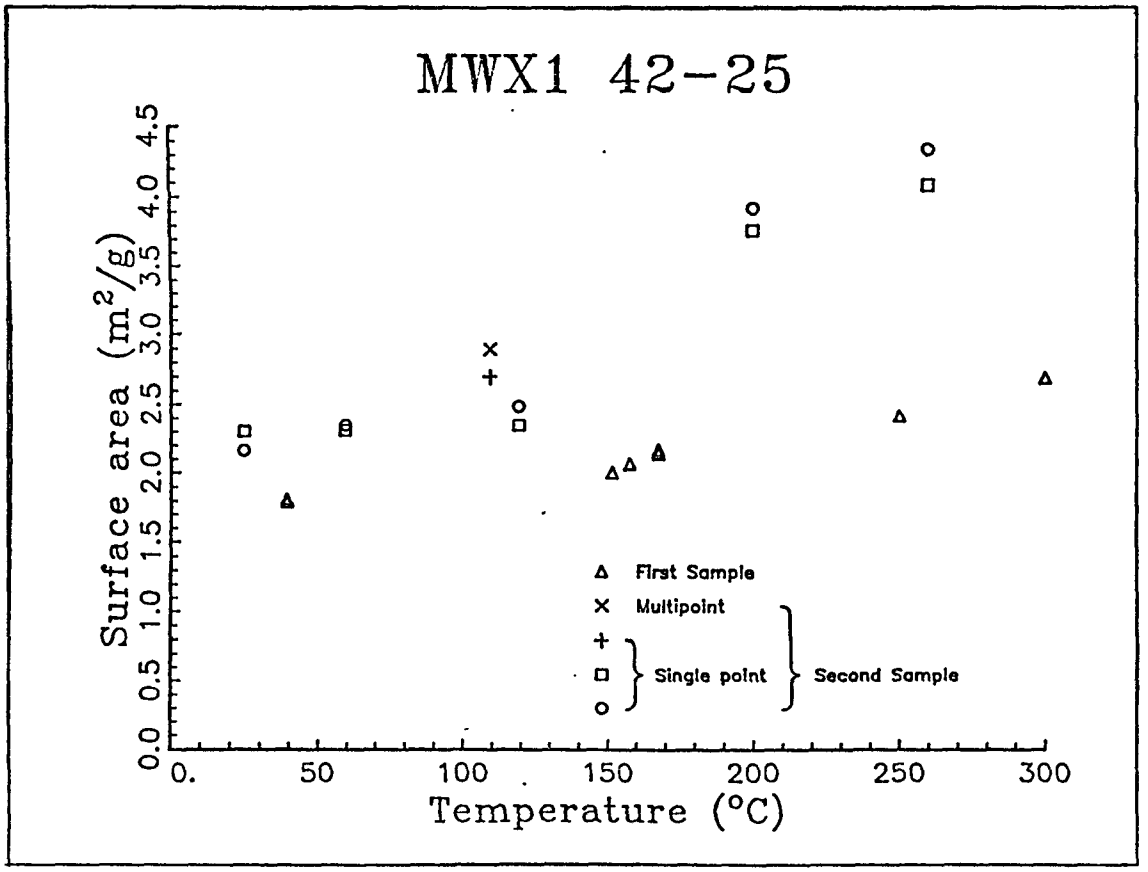

Figure 6. Surface area versus outgassing temperature for crushed sample of MWX1 42-25.

measurements are made by a single-point BET technique. This is a rapid method of obtaining approximate values for surface area based on nitrogen desorption at one partial pressure.

These measurements were made with a partial N_2 pressure of 0.3 using one to two gram, crushed core samples. Samples are outgassed for a minimum of 15 minutes at the lowest temperature in a stream of the 30% nitrogen in helium mixture. Successive cycles of adsorption and desorption show little or no change in surface area, and baseline measurements of gas compositions are very stable, both indicating that the outgassing process is effectively completed.

Use of the single point method presupposes that the partial pressure of nitrogen used for the measurement is in the linear portion of the BET curve and that the intercept of that curve is not far from zero. These assumptions have been validated for a typical tight gas sample by a ten-point adsorption/desorption BET analysis performed by Quantachrome. Fig. 7 shows the BET plot obtained from adsorption for a portion of rock taken from MWX1 42-25 which was passed through a jaw crusher and then a roll crusher. Linearity does extend to the 0.3 partial pressure, and closure of the adsorption/desorption isotherms is at a higher partial pressure, around 0.4, as shown in Fig. 8. Assuming the intercept to be zero and calculating the slope based on the 0.3 partial pressure measurement would result in a value for surface area of 2.7 instead of the multipoint value of 2.9 M^2/g.

The observed single-point surface areas measured in our laboratories for portions of the crushed MWX 42-25 sample were still lower (2.3-2.5 m^2/g) than that calculated from the Quantachrome results, and vary somewhat from one sample to another (Fig. 6). The discrepancy between single and multipoint surface areas may be due to outgassing conditions. Quantachrome outgassed its sample at 110°C in a vacuum, whereas the single point samples were outgassed under the N_2-He mixture. Decreasing pressure may drive off either water or organic compounds which are retained at 110°C and ambient pressure. This observation has important implications for core handling before laboratory measurements and will be investigated further. Overall, the Quantachrome results confirm that the single point method gives a reasonable approximation of surface area for tight gas samples, while pointing out the necessity to consider the effects of sample treatment on this and other measurements.

The possible influence of crushing of rock samples before measurement is shown in Fig. 9. A crushed sample was sieved into four fractions; surface area versus temperature is reported for each fraction and for an unfractionated sample. Differences between the whole sample and the three largest size fractions are small and do not show any trend with size. The only fraction which is distinctly different is the finest (particles less than 0.42 mm in diameter). Since the other sieved fractions do not decrease in surface as compared to the whole sample, it may be that the finest fraction isolates particles in which grinding exposes additional surface. These results suggest that crushing the sample does not significantly change the surface area unless extreme sample segregation takes place.

Increase in outgassing temperature, however, does have a major effect on surface area measurements. We have examples of two distinct types of behavior: most of the Multi-Well samples show increasing surface area as temperature is increased in the range from 25 to 300°C. Several of the coastal samples from

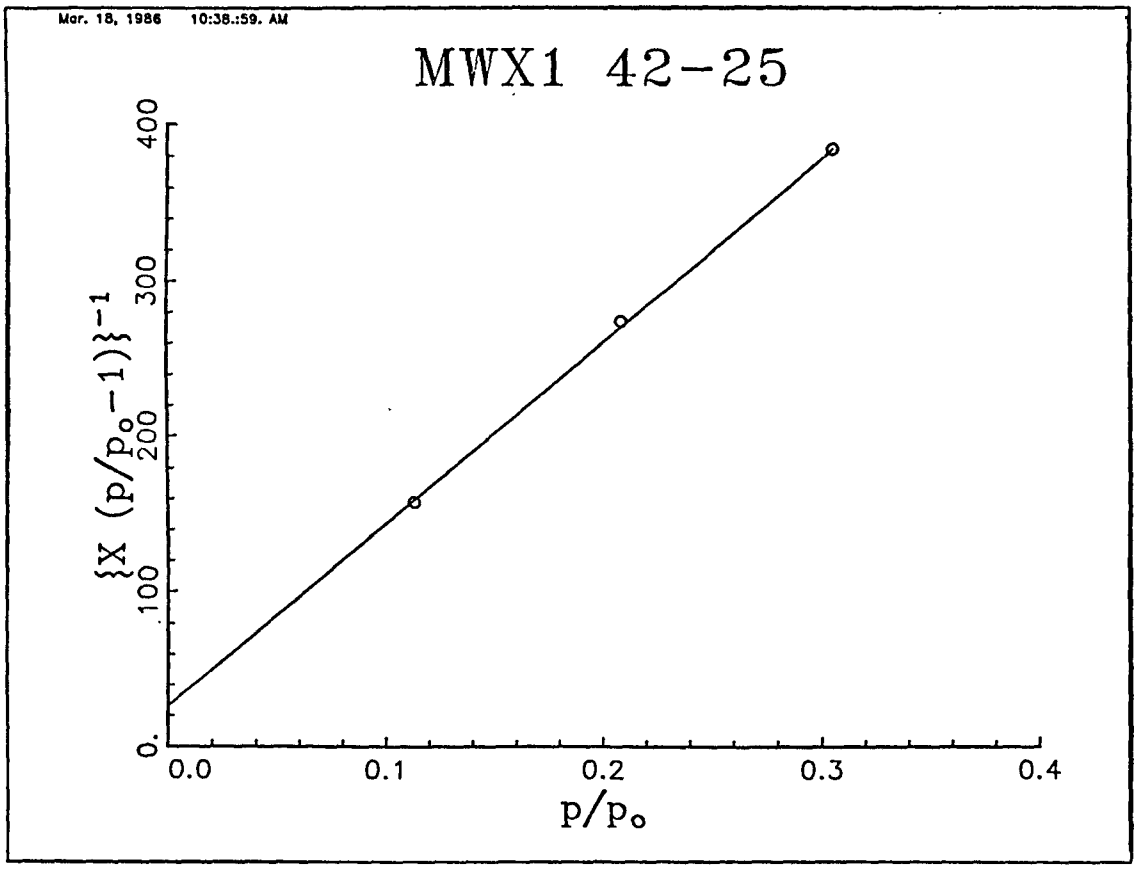

Figure 7. Relationship between nitrogen adsorption and partial pressure (BET plot).

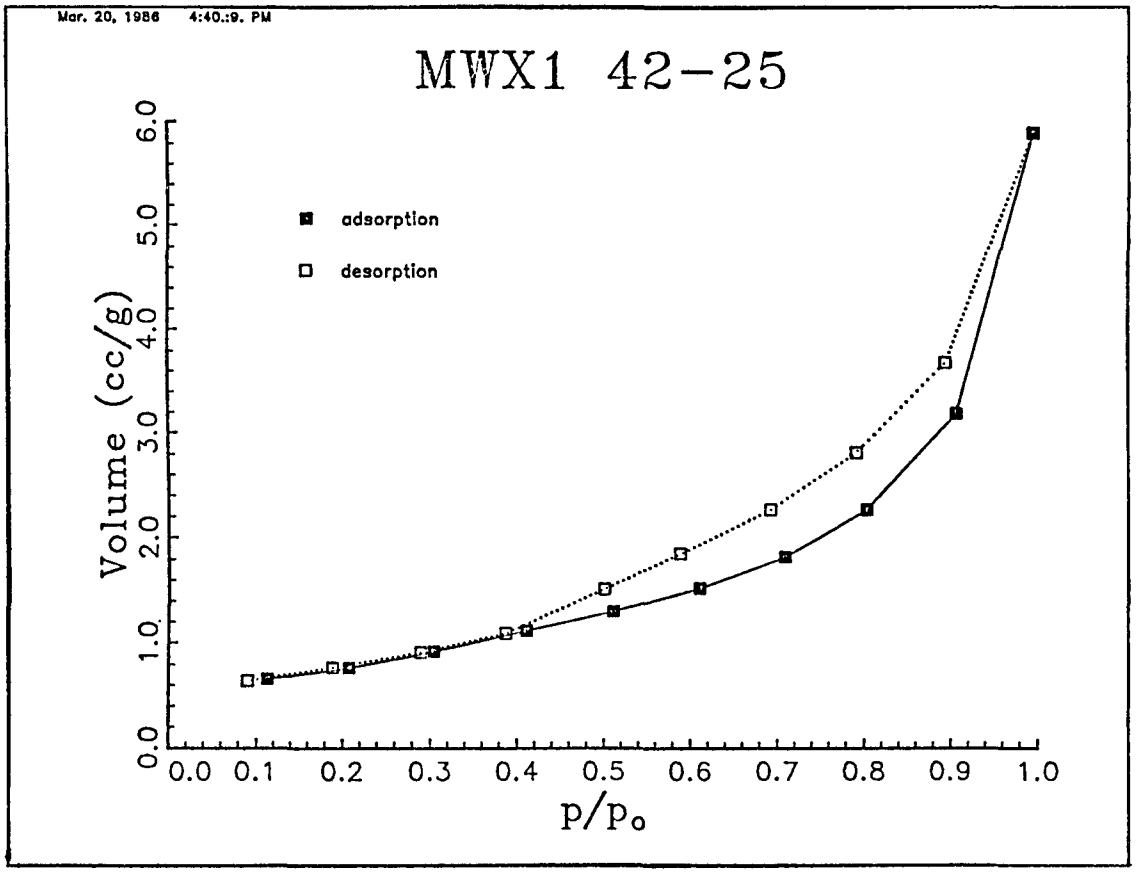

Figure 8. Adsorption-desorption hysteresis loop for nitrogen on MWX1 42-25.

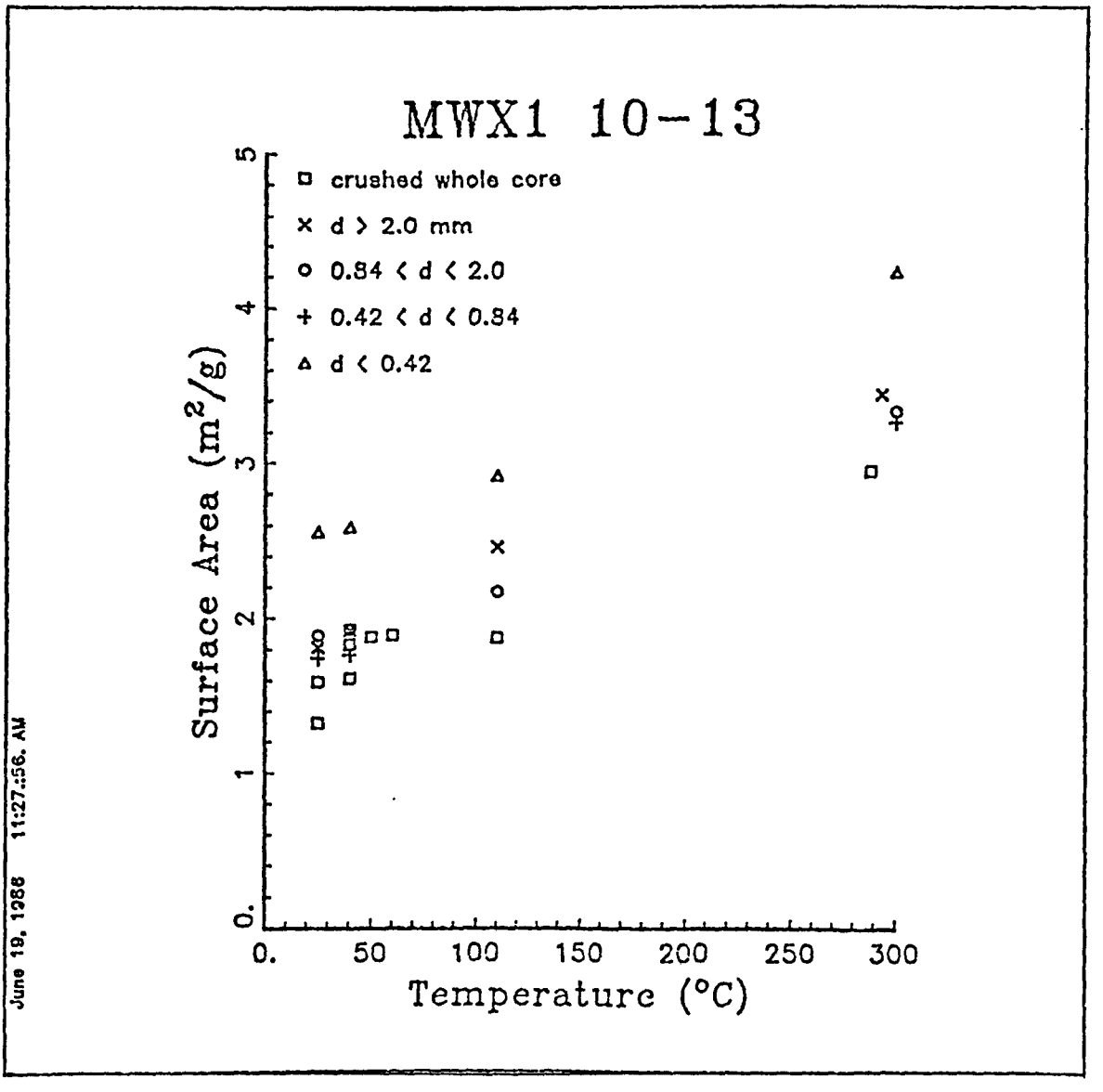

Figure 9. Effects of sample segregation on surface area.

MWX2 showed initial decreases in surface area on heating from 25 to 40°C with small increases as the temperature is raised to 60°C. At temperatures in the range of about 150 to 300°C, the duration of heating becomes an important factor. All samples show maximum surface area immediately following heating followed by small decreases as the sample is allowed to remain at room temperature over a period of hours or days.

(c) Index of Quality of Pore Space From Point Counts on Thin Sections

Primary and secondary pores in sandstones commonly contain remnants of detrital materials and/or authigenic minerals that occlude porosity to various degrees. For tight gas sands this has led to large differences in estimates of porosity from thin sections.[1] Because accurate estimation of void areas within partially filled pores is crucial to petrographic analysis, a more accurate method of assessment of pore quality was devised. By this scheme, points are assigned values (in 25% increments) ranging from 0% for mineral grains to 100% for open voids. Pores containing mineral matter are assigned values of 25%, 50%, or 75%, depending upon extent of porosity occlusion. Evaluation of pores containing finely distributed material, such as clay minerals, is accomplished by estimation of intensity of blue coloration as compared to blue epoxy within open voids. Results obtained by relatively unskilled observers were found to be much less subjective than those obtained by conventional counting techniques.

Table 3 demonstrates that this method gave much improved agreement between laboratory porosity measurements and those obtained by the above point-counting technique. Also the ratio of total number of equivalent voids to the number of count gives a measure of pore quality. For Multi-Well sandstones, pore quality ranges from 0.26 to 0.39 showing that most of the pore space is 75% filled by microporosity.

Also included in Table 3 are values for a carbonate rock, Berea sandstone, and a glass bead pack which provide examples of intermediate- and high-quality porosity. The bead pack, even though it contains no microporosity, does not exhibit a pore quality of 1.0 because thin sections are not infinitely thin. Pores necessarily contain tapered edges of beads that will cause estimation of pore quality to be less than unity. In future work the diagenetic significance of visual porosity counts will be evaluated by distinguishing between partially dissolved detrital grains, partially dissolved cements, and pores which have been partially filled with authigenic minerals.

2. NATURAL FRACTURES IN TIGHT SANDSTONES

Origin of Natural and Artificial Fractures in MWX Sandstones

The nature and origin of fractures in MWX sandstones were analyzed using the following techniques: 1) visual inspection of MWX cores, 2) petrographic examination (all available thin sections), 3) scanning-electron photomicrography, and 4) cathodoluminescence micrography. To date, twenty MWX sandstones containing fractures have been studied.

At least two, and possibly four, episodes of natural fracturing are represented in Mesaverde sandstones at MWX. Calcite-filled fractures are the

Table 3. Pore Quality in Multiwell Sandstones and Other Selected Media

Sample ID	PRRC-Lab Measured Porosity	Thin-Section Porosity	Counts (n=600) Mineral Grain 0%	25%	50%	75%	Clean Pore 100%	Pore Quality
Multiwell Sandstones								
MWX2 48-9	8.3	9.3	438	103	57	2	0	0.34
MWX2 56-19	7.0	5.1	508	68	20	2	2	0.33
MWX2 51-19	7.5	7.7	481	76	35	6	2	0.39
MWX2 52-15	9.7	8.4	425	150	24	1	0	0.29
MWX2 54-11	7.5	8.2	412	179	9	0	0	0.26
MWX2 57-5	5.7	5.6	511	50	34	3	2	0.38
MWX2 55-16	7.2	5.7	480	96	20	0	0	0.29
MWX1 31-32	5.4	4.5	520	54	24	2	0	0.34
MWX1 42-25	7.9	7.9	460	106	20	13	1	0.34
MWX1 14-14	8.0	6.5	482	82	34	2	0	0.33
Carbonate	-	9.0	554	9	38	17	20	0.64
Berea Sandstone	-	20.9	451	7	19	34	89	0.84
Bead Pack	-	36.5	368	0	26	0	206	0.89

most abundant type. These fractures are subvertical, as much as several millimeters in width and trend approximately east-southeast.[3] No remaining thin-section porosity was noted in these fractures, although vuggy porosity associated with large calcite-filled fractures has been noted in some cores.[4]

Cathodoluminescence (CL) microscopy is underway to help further constrain the timing of calcite-filled fractures in Mesaverde sandstones at MWX. Data collected using conventional microscopy suggest that fractures were filled concurrently with the development of intergranular, precompactional calcite cements in the host sandstones, thus indicating that the fractures were formed early in the burial history of the Mesaverde sediments.[5] Preliminary CL microscopy appears to confirm this interpretation, as the luminescence characteristics of fracture fillings are identical to those of the intergranular cements. More CL work will be undertaken in the near future, as well as comparison of stable isotope (O,C) characteristics of the fracture fillings with those of adjacent intergranular cements.

A second generation of fractures was formed after completion of calcite cementation, but prior to development of quartz overgrowths. These fractures are rare (only two examples were noted) and are filled by diagenetic quartz. Residual porosity was noted in one of the quartz-filled fractures.

A possible third generation of fractures is recorded in a few fluvial sandstones. These fractures contain bituminous residue, but the possibility remains that this residue was mobilized into artificial fractures during epoxy injection of the samples. Fractures containing no diagenetic products are common and represent a possible fourth episode of fracturing. However, it seems likely that most or all of these fractures were produced artificially, during coring or thin-section preparation.

Flow Along Mineralized Fractures

Relative permeabilities to nitrogen gas at five different levels of water saturations have been determined for MWX1 29-31 and MWX1 29-7B. Plugs were cut vertically so that the mineralized fracture would run along the length of the sample. Oven-dried plugs were saturated with distilled water under vacuum. The desired level of water saturation was obtained by evaporation. Measurements were made sequentially at 60%, 45%, 30% and 15% water saturations. Core plugs were then oven-dried at 110°C, and gas permeabilities were measured. Results are given in Table 4.

With only few exceptions, the results show the expected trend. Permeability decreases with increase in water saturation. Increase in pressure sensitivity with increasing water saturation is also observed (Figs. 10 and 11). However, the effect of water content on permeability appears to be less prominent at lower confining pressures. For instance, at 60% water saturation, when the overburden pressure is changed to 500 psi, both samples exhibited higher permeabilities than expected, as illustrated in Figs. 12 and 13. This observation is quite contrary to what we have experienced so far. One explanation for this behavior could be that the flow of gas in these two samples is mainly controlled by the mineralized fracture, especially at low confining pressure. Presence of water plus the pressure sensitivity of the rock accounts for the large reduction in permeability at 5000 psi confining pressure. When

Table 4. Relative Permeabilities to Nitrogen Gas at Different Levels of Water Saturation

(a) MWX-1 29-31 V* [5730.9 - 5731.2 ft]

Porosity = 6.95%

Water saturation (%)		I Unloading K_p(μd)			$\frac{K_{500}}{K_{5000}}$
Initial	Final	5000 psi	2000 psi	500 psi	
60	57.15	0.167	1.20	9.68	57.96
45	43.45	0.408	1.38	11.0	26.96
30	29.12	0.875	2.58	16.21	18.53
15	14.49	2.00	4.65	20.44	10.22
0	0	4.44	8.75	26.70	6.01

(b) MWX-1 29-7B V* [5733.2 - 5733.6 ft]

Porosity = 6.14%

Water saturation (%)		I Unloading K_p(μd)			$\frac{K_{500}}{K_{5000}}$
Initial	Final	5000 psi	2000 psi	500 psi	
60	56.91	0.72	3.16	56.56	78.56
45	42.73	1.74	4.43	75.06	43.14
30	28.81	3.54	7.41	88.53	25.01
15	14.27	5.94	11.68	96.82	16.30
0	0	9.33	15.71	104.63	11.21

ΔP = 150 psi

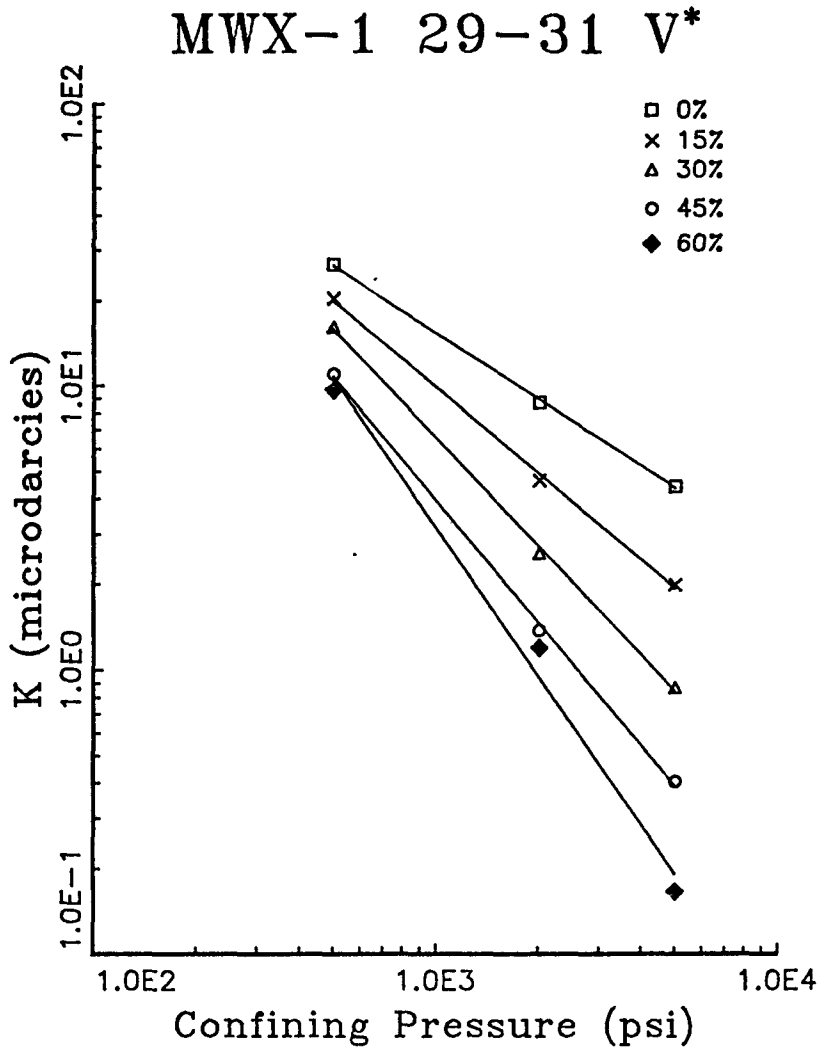

Figure 10. Permeability to gas versus confining pressure at five levels of water saturation.

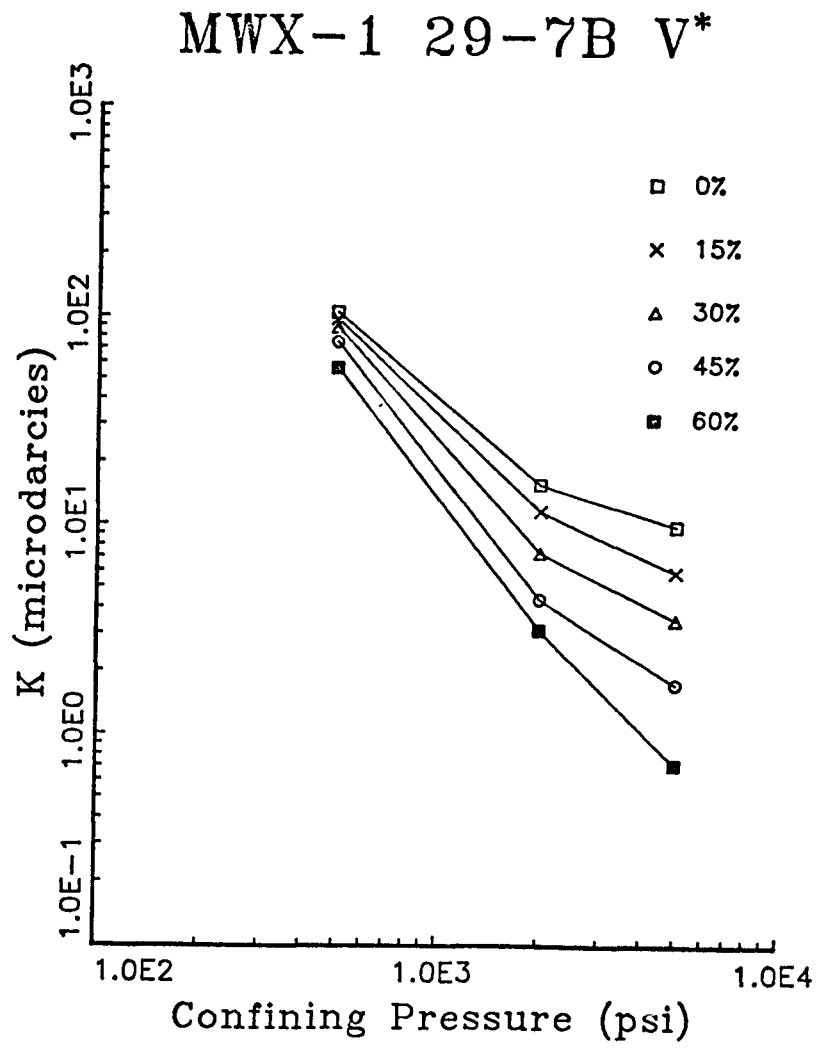

Figure 11. Permeability versus confining pressure at five levels of water saturation.

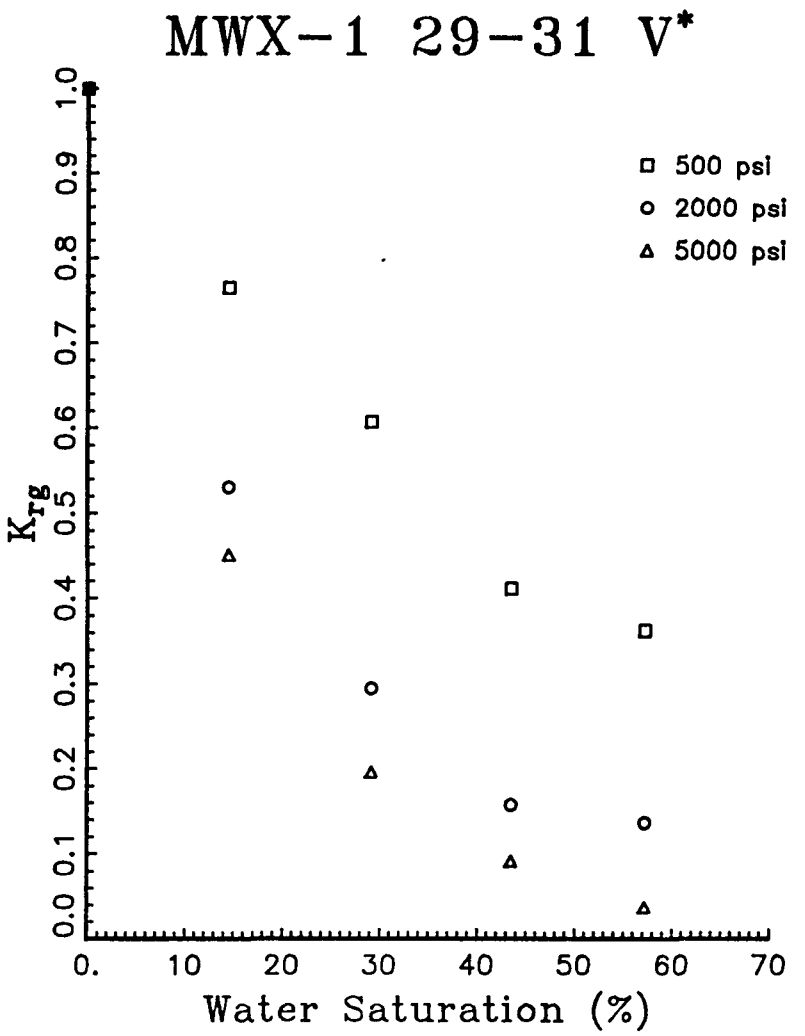

Figure 12. Permeability to gas versus water saturation.

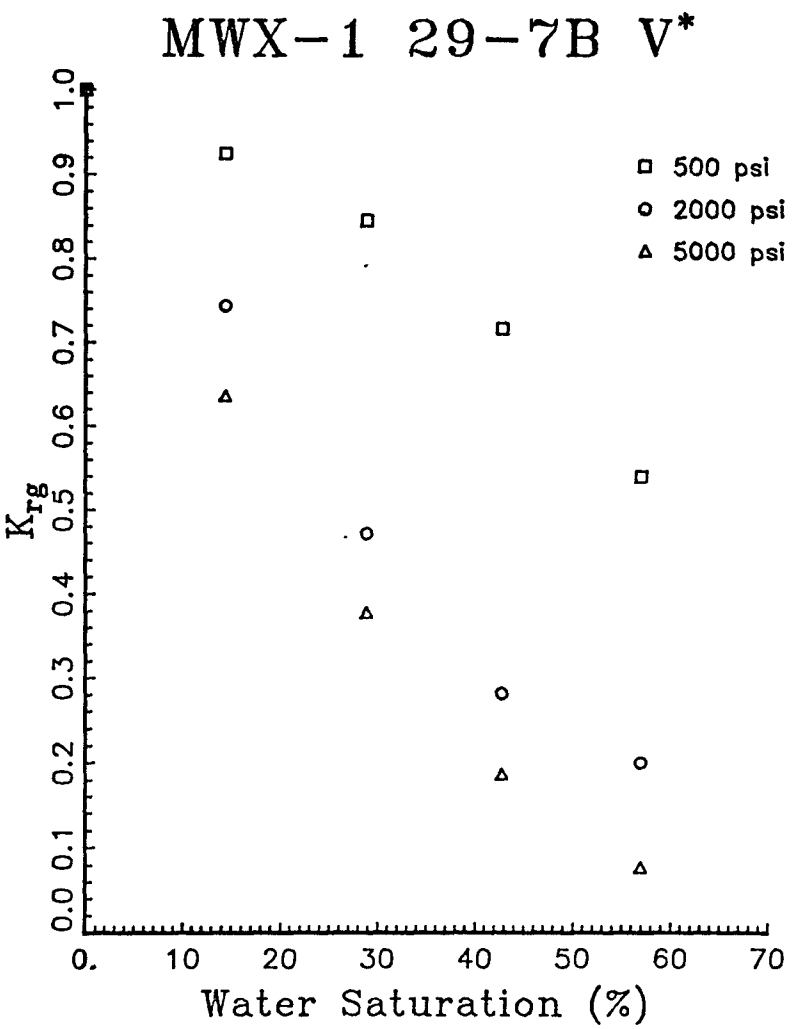

Figure 13. Permeability to gas versus water saturation.

the pressure is lowered to 500 psi, the fracture becomes more conductive than the neighboring matrix.

3. EFFECT OF CORE HANDLING ON PROPERTIES OF LOW PERMEABILITY SANDS

A sealed core sample from MWX3 was provided by Sandia Laboratories for a detailed comparison of permeabilities measured on preserved and dried samples. The sample, designated as MWX3, 42-4 was kept in a high humidity environment after breaking the seal so that initial measurements could be made on a core which had never been allowed to dry. Comparison of the permeabilities measured for such a carefully preserved core with the same sample after deliberate drying should provide much needed information on the extent of damage done to cores by allowing them to dry before laboratory tests are performed.

Several core plugs were cut from the whole core. A sequence of tests was begun on Plug I including measurement of water permeability, relative permeabilities to gas at a series of decreasing established water saturations, drying of the sample, and measurement of an absolute gas permeability, followed by a repeat of the water and relative gas permeability sequence.

Tests of Plug I proceeded through the drying and resaturation steps. The water permeability of the dried sample had been measured when a fracture developed in the sample. One further measurement, relative permeability to gas at 60% water saturation, was completed before another fracture was found. At this point the sequence of tests was discontinued, and a second plug, Plug II, was cut. Again the preserved core was saturated with distilled, deaerated water, and the liquid permeability was measured as a function of confining pressure. These results are shown as open square symbols in Fig. 14. Another preserved core plug (Plug III) was saturated with a brine of 3.55% NaCl, chosen to simulate a brine composition reported by Core Labs for a Multi-Well sample.[6] Open circles show the water permeability as a function of confining pressure for the brine saturated, preserved core samples. Slightly higher permeability is observed for brine than for distilled water at all values of confining pressure.

The permeability to nitrogen gas was measured for Plug II at four intermediate levels of water, 60, 45, 30 and 15%. Beginning with the completely saturated plug, each successively lower saturation was established by allowing water to evaporate slowly from the sample. Only minor changes in saturation have been observed during the course of permeability measurements. Fig. 15. compares the gas permeabilities at each water saturation and confining pressure for Plugs I and II. Also included are the absolute permeabilities to gas measured after drying the core plugs at 110°C until constant weight is attained (S_W = 0%). Remarkable agreement is obtained between the permeabilities for these two adjacent samples at almost all conditions.

After drying and gas permeability measurement, Plug II was resaturated with distilled water, and the water permeability remeasured. The results are shown as filled squares in Fig. 14. For comparison, the brine-filled plug was dried at 110°C, then resaturated, again with 3.55% brine. The brine permeability after the drying step is shown in Fig. 14 as filled circles. Permeabilities to liquid are higher for both plugs after drying and resaturation than for the preserved plugs. However, somewhat less difference is observed between

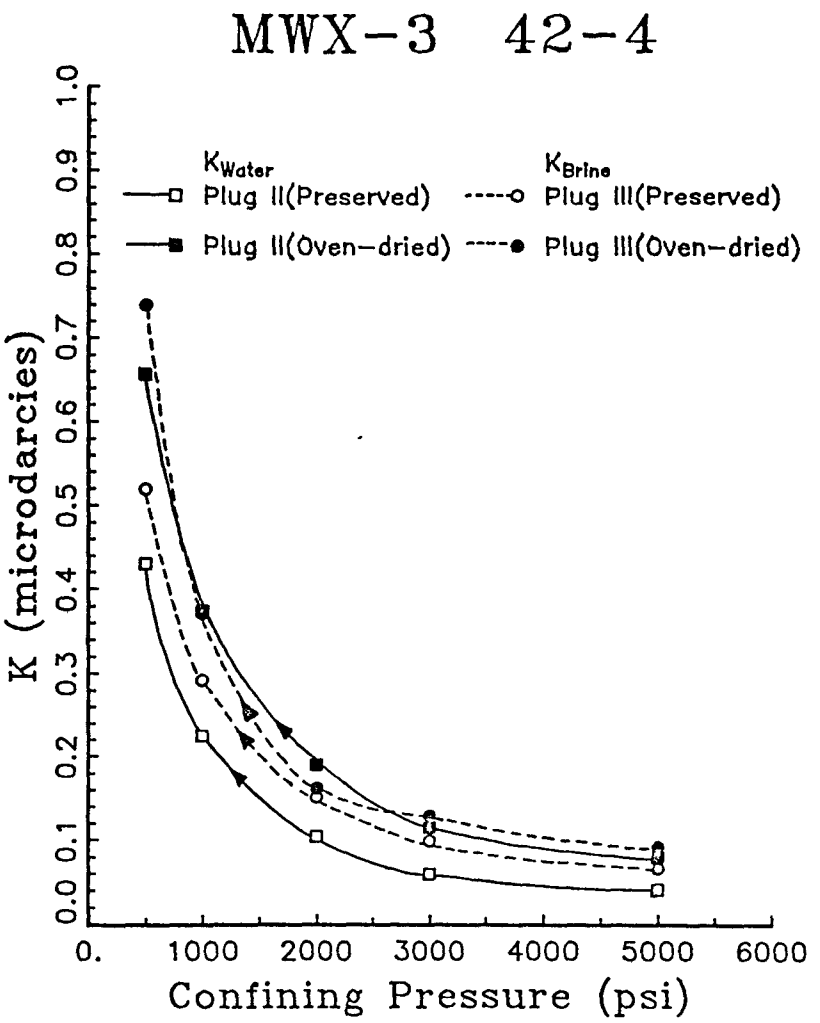

Figure 14. Comparison of water and brine permeabilities.

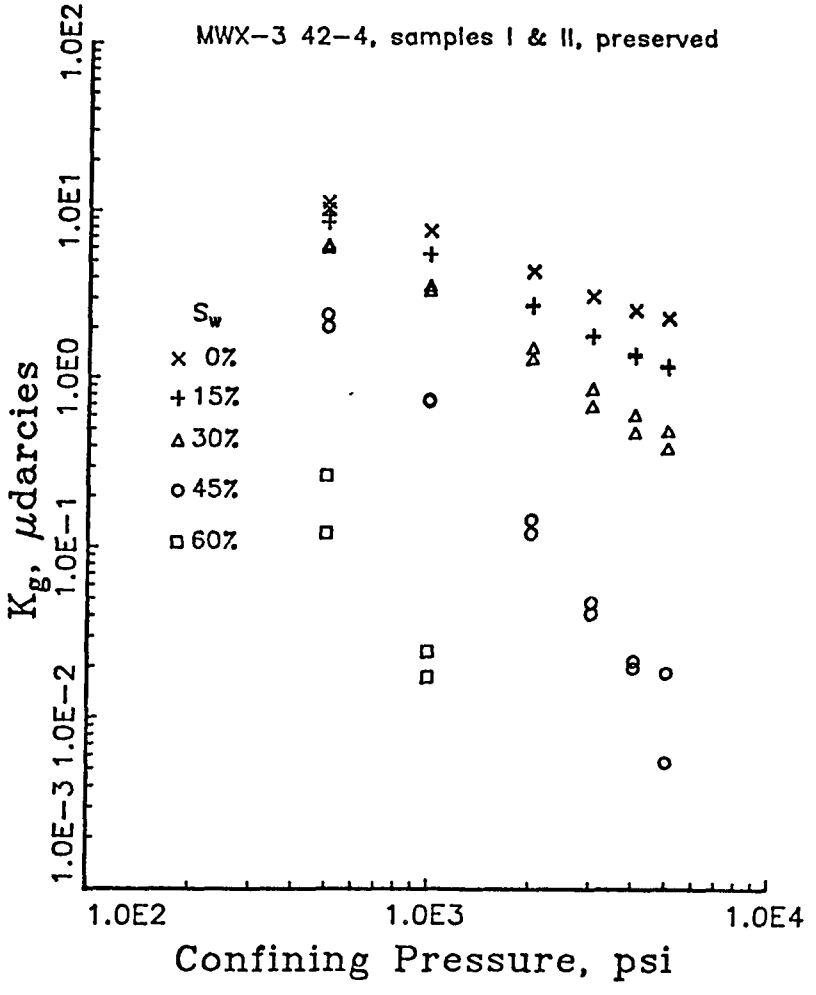

Figure 15. Permeability to gas versus confining pressure of five levels of water saturation for preserved core (duplicate tests).

the two cases for the brine saturated plug than for the distilled water case. This suggests that changes in permeability arising from handling in the laboratory may be exaggerated by measuring with distilled water.

Permeabilities to gas in the presence of water were remeasured for Plug II to observe the changes caused by drying. Fig. 16 compares the permeability as a function of confining pressure for each level of water saturation before and after the drying step. Significant changes in permeability are observed only at the highest confining pressures and water saturations. Fig. 17 shows the relative permeability as a function of water saturation for measurements at 500 and 5000 psi confining pressure. The change in relative permeability with pressure at a given water saturation is very similar for the preserved and dried cases.

The effect of drying on capillary pressures measured by equilibration of samples at constant relative humidity is shown in Fig. 18. An equivalent pore radius or crack thickness can be calculated using the Kelvin equation[2] which helps with interpretation of the results. The desorption experiment is performed first. Once the cores have both reached 20% relative humidity, and the adsorption experiment is begun, the differences between the two samples are less marked.

4. EFFECT OF OVERBURDEN PRESSURE ON PORE STRUCTURE

Resin Injection for Visible, UV Microscopy and Electron Microscopy

Gies[7] recently demonstrated that UV fluorescence provides an extremely useful approach to study of pore structure in low permeability gas sands. Features of microporosity were revealed that were not observable using visible light. Yanguas and Dravis[8] pointed out that petrographers objected to thin sections for which porosity (normally revealed by a blue dye in the resin) could not also be examined by standard means with visible light. They reported a technique for carbonate and siliciclastic rocks using a resin containing both a visible and a UV dye. GCR-331 resin was used with its viscosity reduced by adding a large portion of PSTF Invisible Blue UV dye. However, we found that the addition of hardener (DET) and an ether (BGE) did not thin the resin sufficiently to give good impregnation of the Multi-Well core samples. Furthermore, the resin did not fluoresce well, at least for the wave lengths examined in our UV reflectance system. We have experimented with several types of resins and dyes in finding a suitable low viscosity, blue/fluorescent-dyed resin that would impregnate low permeability sandstones using vacuum and high pressure injection.[5,10] Once impregnated, the effect of overburden pressure was to be investigated by applying 5000 psi confining pressure to the core sample. The resin would then be cured by heating the core holder in a water bath.

Preparation of pore casts and thin sections of low permeability sandstones requires impregnation of samples by a resin. Ideally the resin should have the following properties:

1. low viscosity for penetration,
2. blue coloration for examination with visible light,
3. UV dye for examination by UV fluorescence,

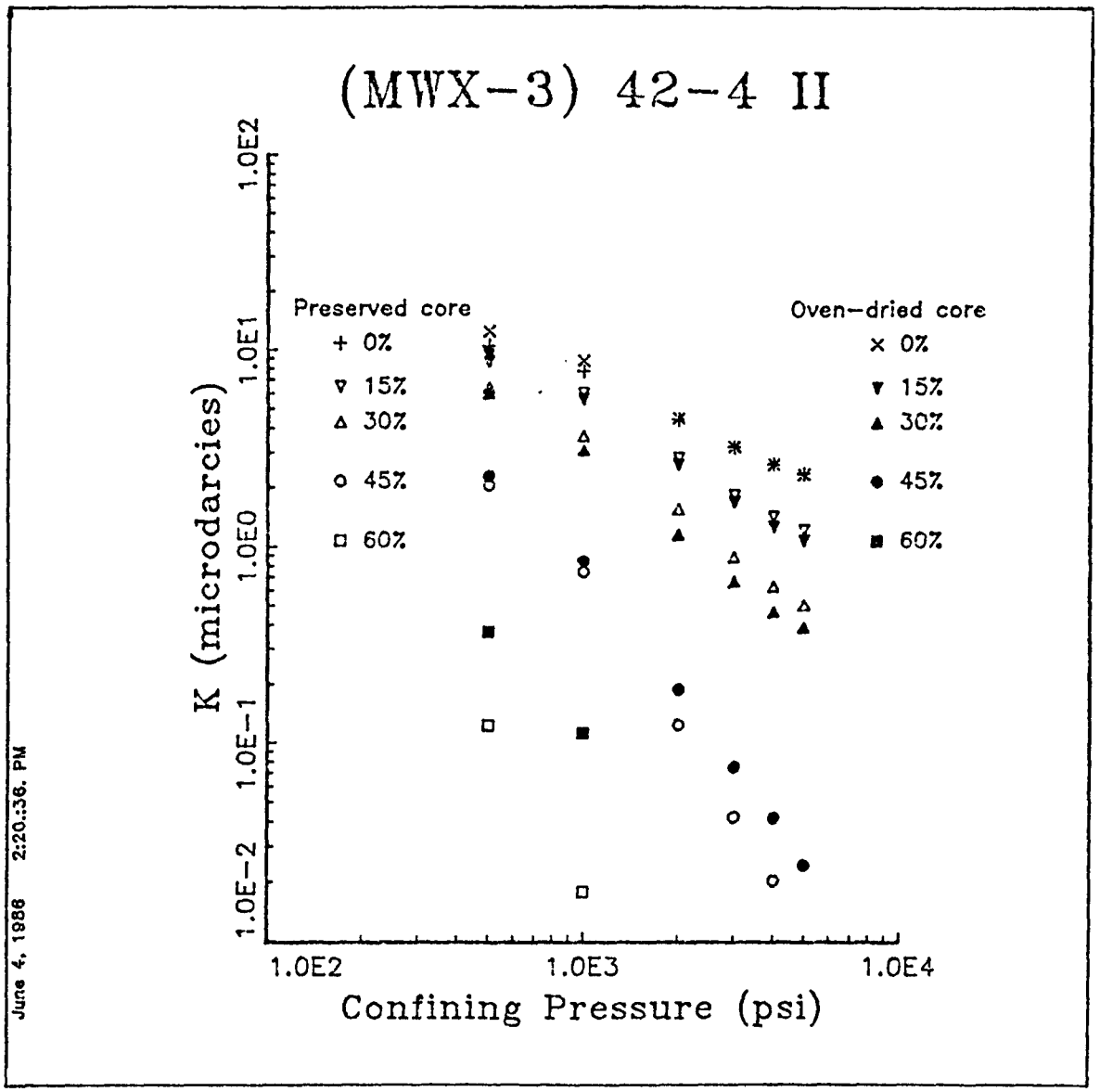

Figure 16. Gas permeability versus confining pressure at different levels of water saturation for preserved and oven-dried MWX3 42-4.

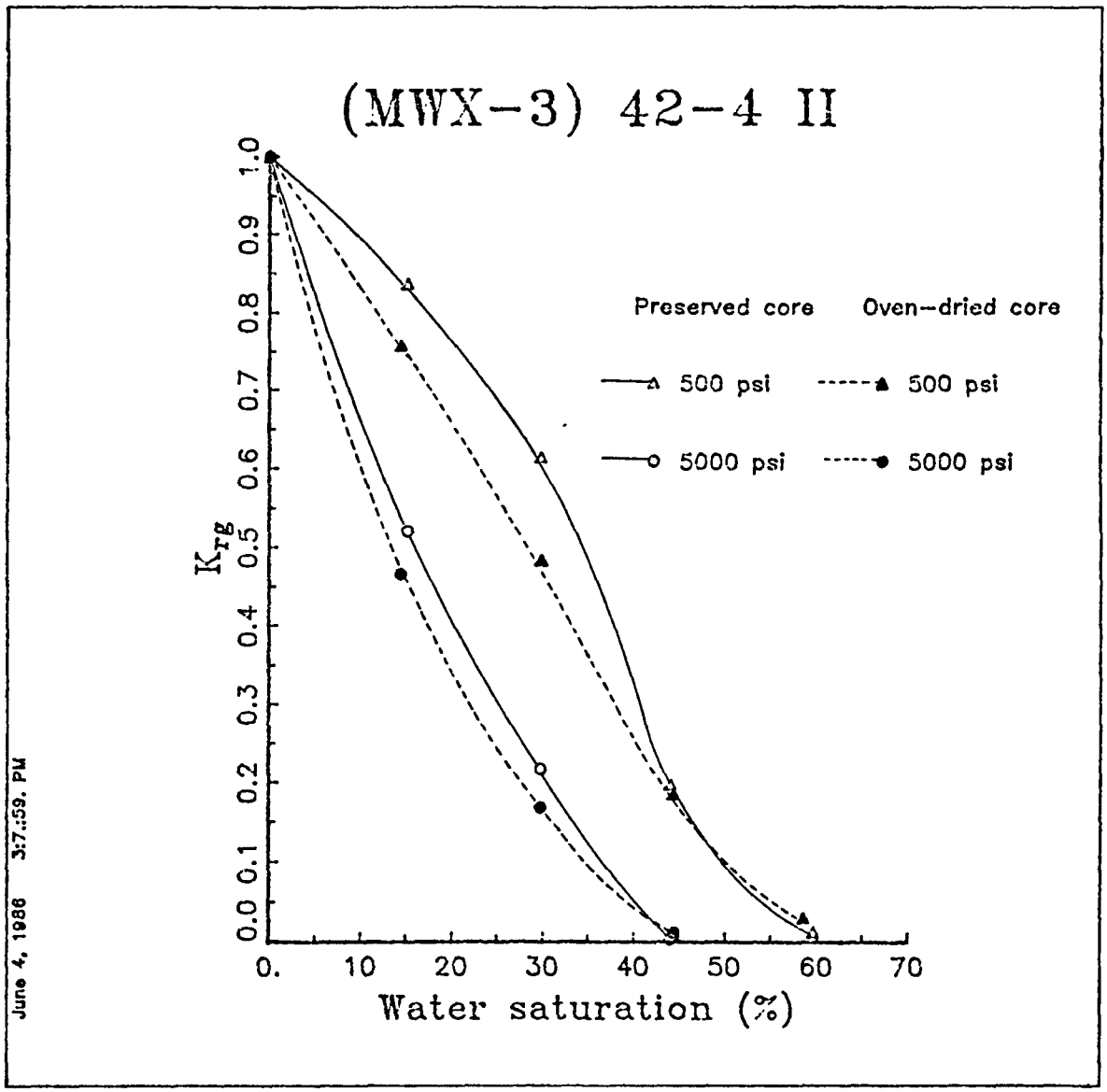

Figure 17. Relative permeability to nitrogen as a function of established water saturation at confining pressures of 500 and 5000 psi for preserved and oven-dried MWX3 42-4.

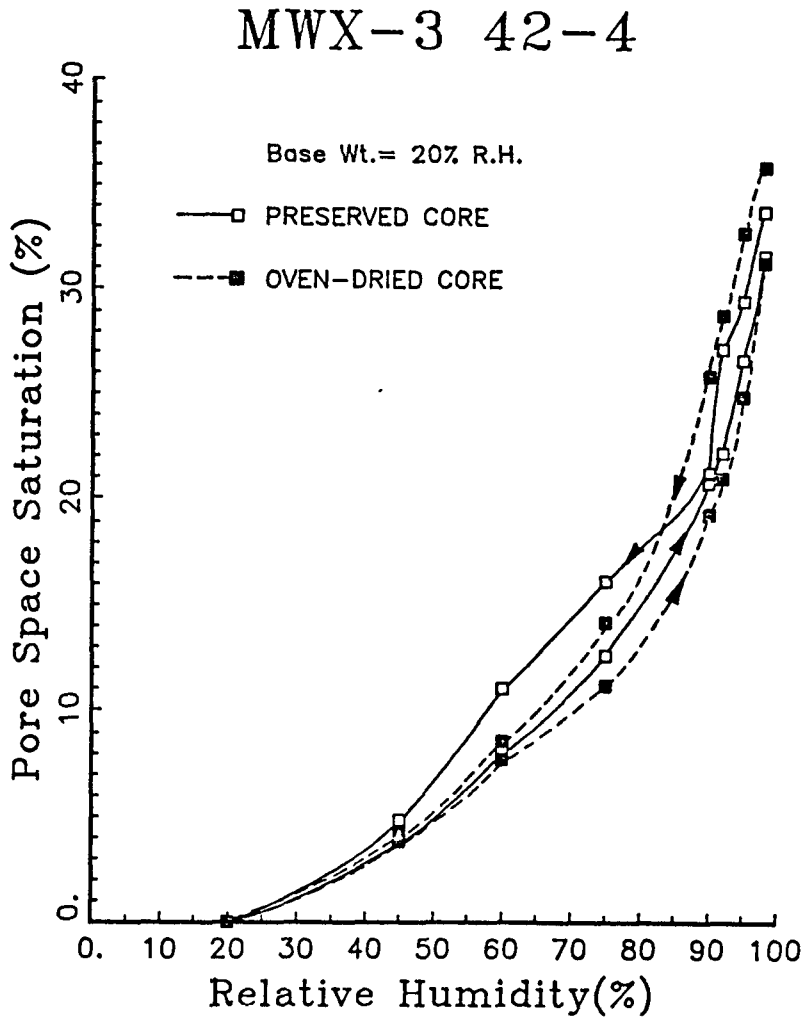

Figure 18. Desorption-adsorption isotherms for MWX3 42-4 (base weight at 20% relative humidity and 25°C).

4. must not harden too quickly or too slowly - suitable for obtaining solidification after application of confining pressure,
5. minimum shrinkage on solidification,
6. chemical resistance to hydrofluoric and other acids used in preparation of pore casts, and
7. sufficient hardness for preparation of thin sections.

Considerable effort was also expended in using styrene monomer and a combination of dyes but results were generally unsatisfactory.[5,10]

Numerous resins were tested. Best results for penetration and hardness were obtained with the Spurr Low-Viscosity resin. Thin sections of the required quality were made with the dyes, Nile Blue A and Fluor Yellow. A strange feature of this mixture, however, was that although excellent quality of blue color was obtained under visible light within the sample, the surrounding resin was uniformly brown in appearance. This poses a serious problem if it occurs within the sample, because it will be difficult to distinguish resin from lithic fragments. Impregnation of Berea sandstone (at least 10,000 times more permeable than the tight sandstones) resulted in brown coloration within the pore space. Further tests were performed to identify a suitable combination of dyes for use in the Spurr resin. Oil Blue M gave good color with visible transmitted light, but the sample did not fluoresce as strongly as desired. Comparison of thin sections in which the injection resin was setup with the core at (a) ambient conditions, (b) 5000 psi confining pressure, indicated that sheet pores at grain boundaries tended to be close with application of overburden pressure.

SUMMARY AND FUTURE WORK

Further work on advanced core analysis has been performed on 35 whole core matrix samples. Measurements included porosity, surface areas, adsorption isotherms, x-ray diffraction, mineral analysis from thin sections, pore casts and measurements of Klinkenberg permeabilities (k_∞) at confining pressures ranging from 500 to 5000 psi. Results showed porosities ranging from 3 to 12%, surface areas from 0.97 to 4.35 m^2/g, and permeabilities ranging from 0.026 to 44.3 μd at 5000 psi confining pressure. Pore size and change in pore size with confining pressure were determined from the slopes of Klinkenberg plots. The tested cores showed wide variation in sensitivity of permeability to confining pressure with the ratio of $k_{\infty,500}$ to $k_{\infty,5000}$ for first unloading ranging from 1.5 to 45. These initial results served as a screening test for selecting cores for more detailed study of the causes of pressure sensitivity and the superimposed effects of water saturation.

Several aspects of microporosity in low permeability gas sands have been investigated during the past year. These include measurements of surface area by nitrogen adsorption, adsorption-desorption isotherms, and comparisons of porosity from thin sections with those determined by conventional core analysis. A new approach to measuring the quality of pore space of reservoir rock has been developed from a modified technique for point counting visible porosity in thin sections.

Considerable effort has been expended on development of satisfactory techniques of resin injection. In general, thin sections prepared by commer-

cial organizations did not give uniform penetration or distribution of color. A resin formulation has been developed which has low viscosity for good penetration and contains visible and UV dye so that thin sections can be examined by transmitted visible light and by UV reflectance. Comparison of thin sections in which injected resin was set up with the core at (a) ambient conditions and (b) high overburden pressure indicated that sheet pores at grain boundaries tended to close with application of overburden pressure.

Advanced core analysis has also been carried out on naturally fractured cores because it is suspected that fractures sometimes provide paths of high permeability which will permit gas to flow more readily from the matrix rock to the wellbore. Multi-Well cores which have mineralized fractures are usually obvious because the fractures are vertical and filled with calcite. Eleven cores containing mineralized fractures have been selected for detailed study of flow along and across the fractures and for application of specialized techniques for determining flow distribution. Two of the fractured cores were selected for measurement of relative permeabilities to gas for cores having the healed fracture running along its length. Measurements were made at three levels of overburden pressure and five levels of water saturation. In general, results for the fractured cores are fairly similar to those obtained for the rock matrix. Also during the past year the timing of fracture events with respect to diagenetic history has been investigated.

Application of high speed centrifuge and desorption isotherms for determination of drainage capillary pressures to very high values has been continued. Permanent damage caused by drying was assessed by comparing water permeabilities for fresh cores (cores which were stored to prevent evaporation) with the same cores after they had been allowed to dry. Permeabilities for cores which had been dried were higher than for fresh cores but the differences were fairly minor.

PROPOSED WORK FOR YEAR 3

Task 1. Advanced Core Analysis

Reliable core analysis techniques are essential to proper formation evaluation. The results are important to interpretation of the production behavior of tight sands and to their commercialization. Detailed study is being made of 35 core samples in all, and much of this work is complete. Primary objectives of work on low permeability gas sands at the Center as started at the request of the U.S. Department of Energy was to conduct a research program aimed at understanding the properties and flow behavior of low permeability gas sands. Discussion of the importance of low permeability gas sands to New Mexico and the nation as a whole is discussed in Section 7 of the proposal.

A unique opportunity to carry out this research in conjunction with a field project came with advent of the MWX field experiment. Core taken during the course of this project from three wells is being tested in the work on advanced core analysis work. Tight sandstones can exhibit very high sensitivity of permeability to overburden pressure which is anomalous with respect to conventional reservoir rocks. The tests core samples exhibited decrease in

permeability ranging from 1.5 up to 45 times with increase in overburden pressure from 500 psi to 5000 psi. Thus the samples in total exhibit a wide range of pressure sensitivity behavior.

In previous work, correlations were tested between pressure sensitivity and measured rock properties.[11] It was concluded that details of pore structure related to diagenetic changes appear to be of much greater significance to pressure sensitivity than mineral composition. Direct observation of changes in pore structure with increase in overburden pressure are being attempted for cores impregnated with a low viscosity resin. This work is a logical extension of previous work.

Work to be performed under Task 1 will include:

(a) An account of the diagenetic history of MWX sandstones as it relates to pore structure.

(b) Test for correlations between pressure sensitivity and diagenetic history for at least 30 samples.

(c) Further development of a low viscosity resin formulations containing visible and UV dye for impregnation of tight sands. Use of such resins in tests of the effect of overburden pressure on pore structure through UV microscopy for at least two samples at two levels of confining pressure, one being 5000 psi.

Task 2. Natural Fractures

Multi-Well core shows numerous small tectonic fractures that have become filled by calcite cement. Flow measurements show that these fractures have about the same permeability as the surrounding matrix. Chemical treatment of calcite-filled fractures offers one approach to permeability enhancement.

Work to be performed under Task 2 will include:

Under Task 2, the effect of chemical treatment on calcite-filled fractures will be measured for two samples for at least three levels of overburden pressure. This work will largely complete previous work on natural fractures performed under Phases I and II. A topical report on this subject will be prepared.

Task 3. Investigation of Pore-Filling Cements and the Effect of Chemical Treatments on Core Properties

Effects of Chemical Treatments on Rock Properties

Preliminary studies have been completed on the effect of chemical treatments on rock permeability. This work is mainly aimed at determining which mineral constituents occupy critical positions in the rock pore structure with regard to gas flow and pressure sensitivity. They may also indicate conditions under which tight gas sands can be stimulated by chemicals.

Work to be performed under Task 3 will include:

Under Task 3, results will be obtained for at least six chemical reagents which can be expected to have differing effects on rock permeability. At least two samples of distinctly different deposition of history (marine and fluvial) will be tested. In cases where reagents have significant effect (such as sodium hydroxide on coastal samples), the effect of increase in temperature on permeability will be investigated. This will be an area of special focus during Phase III.

Task 4. Effect of Water on Gas Production

Examples have been reported in which pore structure involving firing clays can be severely damaged by drying. Pore space in low permeability sandstones is largely associated with fire structure (as, for example, revealed by adsorption isotherms). Tests on preserved cores (sealed after recovery to prevent drying) were compared with those obtained after drying.

Work to be performed under Task 4 will include:

Under Task 4, results obtained to date show that gas permeabilities from preserved reservoir core samples (not allowed to dry after recovery) are somewhat lower than for conventional cores (i.e., cores which have been allowed to dry after recovery). Measurements will include absolute permeabilities to gas and brine, and relative permeabilities to gas for at least four levels of water saturation and two levels of overburden pressure. Measurements on the last remaining preserved MWX core specimen will largely complete this part of Task 4.

REFERENCES

1. Morrow, N.R., Ward, J.S., and Brower, K.R., "Rock Matrix and Fracture Analysis of Flow in Western Tight Gas Sands," 1985 Annual Report to the U.S. Department of Energy, DE-AC21-84MC21179, Feb. 1986.

2. Ward, J.S. and Morrow, N.R., "Capillary Pressures and Gas Relative Permeabilities of Low Permeability Sandstone," SPE 13882 presented at the 1985 SPE/DOE Symposium on Low Permeability Reservoirs, Denver, CO, May 19-22, 1985; SPE Formation Evaluation, In press.

3. Verbeek, E.R. and Grant, M.A.: "Fracture Studies in Cretaceous and Paleocene Strata in and Around the Piceance Basin, Colorado: Preliminary Results and Their Bearing on a Fracture-Controlled Natural-Gas Reservoir at the MWX Site," U.S. Geological Survey Open File Report 84-156 (1984).

4. Lorenz, J.C., personal communication (1986).

5. Morrow, N.R., Ward, J.S., Brower, K.R., and Cather, S.M.: "Rock Matrix and Fracture Analysis of Flow in Western Tight Gas Sands," PRRC 86-6, New Mexico Petroleum Recovery Research Center, quarterly report prepared for the U.S. Department of Energy (1986) 1-18.

6. Core Labs Report SCAL 203-840040, August 20, 1984.

7. Gies, R.M.: "An Improved Method for Viewing Micropore Systems in Rocks with the Polarizing Microscope," SPE 13136 presented at the 1984 SPE Technical Conference and Exhibition, Houston, Sept. 16-19.

8. Yanguas, J.E. and Dravis, J.: "Blue Fluorescent Dye Technique for Recognition of Microporosity in Sedimentary Rocks," J. Set. Pet. (1985) 55, 600.

9. Morrow, N.R., Ward, J.S., Brower, K.R., and Cather, S.M.: "Rock Matrix and Fracture Analysis of Flow in Western Tight Gas Sands," PRRC 86-6, New Mexico Petroleum Recovery Research Center, quarterly report prepared for the U.S. Department of Energy (1986) 1-18.

10. Morrow, N.R., Ward, J.S., Brower, K.R., and Cather, S.M.: "Rock Matrix and Fracture Analysis of Flow in Western Tight Gas Sands," PRRC 86-11, New Mexico Petroleum Recovery Research Center, quarterly report prepared for the U.S. Department of Energy (1986) 1-19.

11. Kilmer, N.H., Morrow, N.R., and Pitman, J.K.: "Pressure Sensitivity of Low Permeability Sandstones," J. Pet. Sci. & Eng. (1987) In press.

DOE/MC/21179-2335 ROCK MATRIX AND FRACTURE ANALYSIS OF FLOW IN WESTERN TIGHT GAS SANDS DOE